# Synthesis of nano-sized β-tricalcium phosphate via wet precipitation

Bahman Mirhadi[1], Behzad Mehdikhani[2,*], Nayereh Askari[1]

[1]*Imam Khomeini International University, Engineering Department, Qavin, Iran*
[2]*Institute of Standard and Industrial Research of Iran, Ceramic Department, Karaj, Iran*

Received 29 September 2011; received in revised form 20 October 2011; accepted 5 December 2011

**Abstract**

*Nano-size β-tricalcium phosphate powders with average grain size of 50 nm were prepared by the wet chemical precipitation method with calcium nitrate and diammonium hydrogen phosphate as calcium and phosphorus precursors, respectively. The pH of the system was maintained at 8 and 10.8 by adding of sodium hydroxide. Filtered cake was dried at 80°C and calcined at 700°C. The dried and calcined powders were characterized using X-ray diffractrometry (XRD), Fourier transform infrared spectroscopy (FTIR), inductively coupled plasma atomic emission spectroscopy (ICPAES) and scanning electron microscopy (SEM).*

***Keywords****: biomaterial, β-tricalcium phosphate, wet chemical precipitation, characterization*

## I. Introduction

β-tricalcium phosphate [β-$Ca_3(PO_4)_2$] (β-TCP) and hydroxyapatite [$Ca_{10}(PO_4)_6(OH)_2$] (HA) powders are widely applied in the biomedical fields because of their biocompatibility and osteoconductivity [1,2]. HA is thermodynamically the most stable phase in physiological conditions and has the ability for direct chemical bonding to the bone, while β-TCP is found to be resorbable in vivo with new bone growth replacing the implanted β-TCP [3,4]. Tricalcium phosphate is one of the most important biomaterials based on phosphates, currently recognized as ceramic material that significantly simulates the mineralogical structure of bone [5–8].

TCP has three polymorphic forms: β, α and α′. The latter is of no interest because it transforms into the α-form during cooling. β-TCP is stable at room temperature and reconstructively transforms at 1125°C into α-TCP, which is metastably retained until room temperature during the cooling [9,10].

β-TCP is the low-temperature phase in the CaO-$P_2O_5$ phase diagram. As it was mentioned, β-TCP transforms to α-TCP at 1125°C and above this, up to 1430°C, α-TCP is a stable phase. Above 1430°C, the super α-TCP form becomes stable until the melting point of 1756°C. The ideal Ca/P ratio of β-TCP is 1.5 and the theoretical density is 3.17 g/cm$^3$ as reported by Guelcher and Hollinger [11].

Often tribasic calcium phosphate is mistaken for β-tricalcium phosphate. According to Metsger *et al.* [12], tribasic calcium phosphate is a nonstoichiometric compound often bearing the formula of hydroxyapatite [$Ca_{10}(PO_4)_6(OH)_2$]. TCP is a resorbable temporary bone space filler material. When implanted, TCP will interact with body fluids and form HA in accordance with the following equation:

$$4Ca_3(PO_4)_2 + 2H_2O \rightarrow Ca_{10}(PO_4)_6(OH)_{2\,(surface)} + 2Ca_2 + 2HPO_4^{2-} \quad (1)$$

The reaction rate will decrease with increasing pH of the local solution and further increase the solubility of TCP.

Theoretically, resorbable TCP is an ideal implant material. After implantation, TCP will degrade with time and be replaced with natural tissues. It leads to the regeneration of tissues instead of their replacement and so solves the problem of interfacial stability [11,12]. β-TCP powders are reportedly prepared by liquid-solution methods, such as sol-gel, hydrothermal, micro emulsion and precipitation, as well as gas phase reactions [13–15].

Synthesis of calcium phosphate nanopowder is relevant in biological fields, because the dimensions of large biomolecules such as proteins and DNA as well as those of many important subcellular structures fall in the size

* Corresponding author: tel: +98 91 26417516
fax: +98 24 13230496, e-mail: *mehdikahni.engineer@gmail.com mirhadi@ikiu.ac.ir*,

range between 1 and 1000 nm [16,17]. In the present research work, a wet chemical reaction such as the precipitation method was carried out to prepare β-TCP.

## II. Experimental

*2.1. Powder synthesis*

Detail procedure and experimental conditions for preparation of β-TCP powder by wet chemical process is shown in Fig. 1. β-TCP nanopowders were synthesized by the reaction of calcium nitrate tetra-hydrate ($Ca(NO_3)_2 \times 4H_2O$, 98%, Merck) with diammonium hydrogen phosphate ($(NH_4)_2HPO_4$, 99%, Merck). Briefly, 500 mL of 0.4 mol $(NH_4)_2HPO_4$ solution with pH = 4 was vigorously stirred at room temperature, and 500 mL of 0.6 mol $Ca(NO_3)_2$ with pH = 7.3 was added drop wise over 150–200 min to produce a white precipitate. Throughout the mixing process the pH of the system was maintained at pH = 8 (sample A) and pH = 10.8 (sample B) by adding of 0.1 M sodium hydroxide (NaOH, 99%, Merck). The obtained white suspension was then stirred for 12 h. The synthesized precipitate was washing with distilled water and then with 100% ethanol to improve the dispersion characteristics. The suspension was filtered in a filter glass with application of mild suction. After filtration the compact, sticky filter cake, was dried at 80°C for 24 h. The as-dried powders were crushed by using mortar and pestle and calcined in alumina crucible at 700°C for 2 h.

*2.2. Characterization*

Evaluation of crystalline phases was investigated by X-ray diffractometer (Siemens, model D-500) using CuKα radiation. Silicon powder was used as the standard material for semi-quantitative analysis of precipitated phases. The mean crystallite size ($D$) was calculated from the XRD line broadening measurement from the Scherrer equation [18]:

$$D = 0.89\,\lambda / \beta \cos\theta \qquad (2)$$

where $\lambda$ is the wavelength of the used Cu Kα radiation, $\beta$ is the full width at the half maximum of the β-TCP line and $\theta$ is the diffraction angle.

Infrared spectra were performed by FTIR Bomem (model MB100, Quebec, Canada) in 400–4000 $cm^{-1}$ wavenumber region. For infrared spectroscopy, samples were pulverized and mixed with a given amount of potassium bromide (KBr) and pressed in very thin tablets.

The Ca/P ratio of the dried powder was measured by inductively coupled plasma (ICP) atomic emission spectroscopy (model Varian). No differences were observed in the Ca/P values between the as-dried and calcined powders.

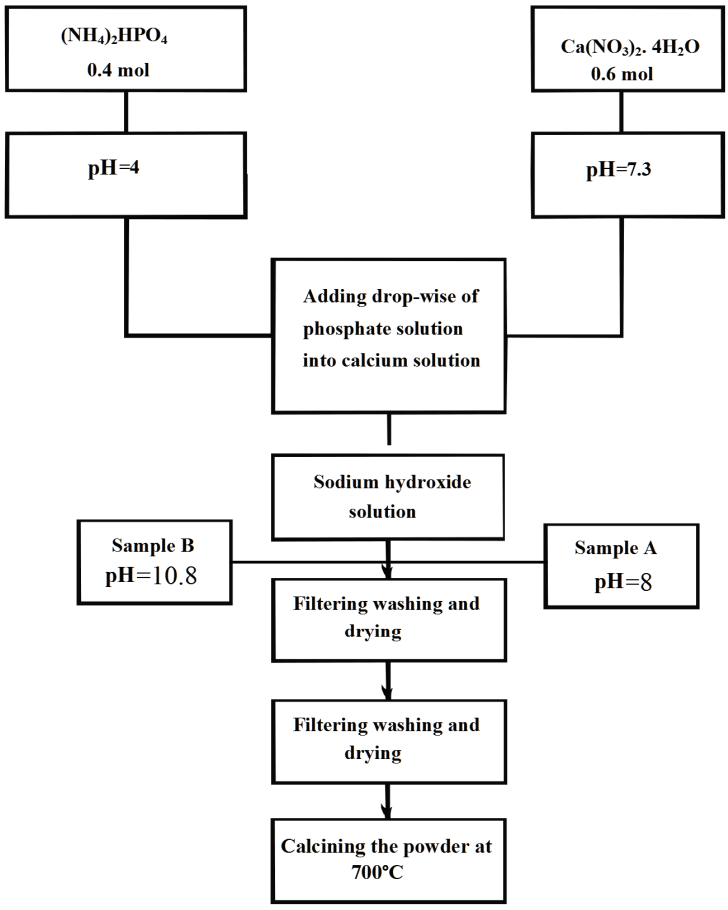


**Figure. 1. Flowchart of wet-chemical precipitation process used for synthesis of β-TCP bioceramic powders**

**Table 1. The ICP analysis of the prepared β-TCP powders**

| Sample | pH | Ca [wt.%] | P [wt.%] | Ca/P atomic ratio |
|---|---|---|---|---|
| Sample A | 8 | 39.81 | 20.43 | 1.51 |
| Sample B | 10.8 | 39.87 | 19.43 | 1.59 |

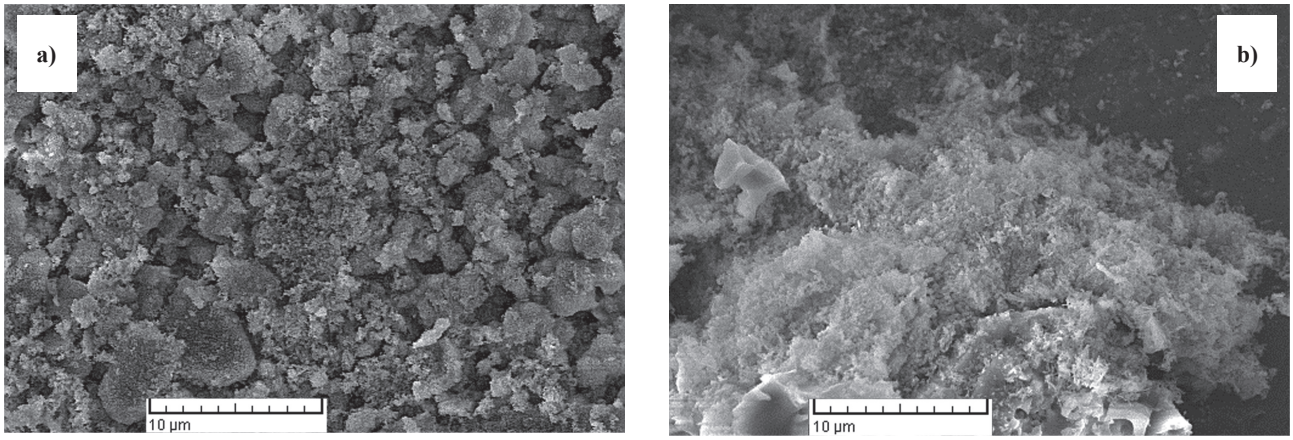


**Figure 2. SEM photomicrographs of as-prepared β-TCP nanopowders (after filtering): a) pH = 8 and b) pH = 10.8**

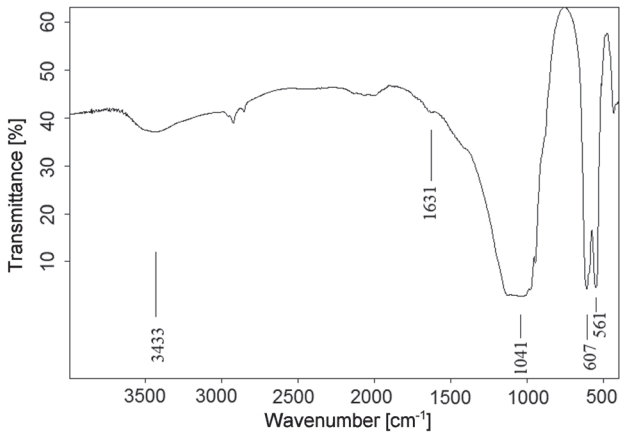


**Figure 3. FTIR spectrum of sample A, synthesized at pH = 8**

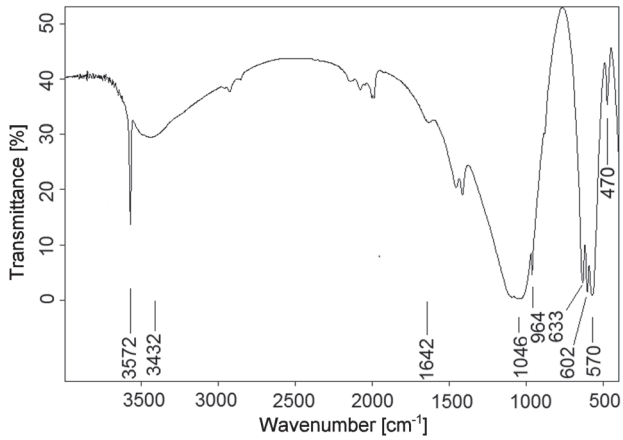


**Figure 4. FTIR spectrum of sample B, synthesized at pH = 10.8**

Structure and morphology of the investigated samples were examined by scanning electron microscopy (SEM, VEGA-TESCAN).

## III. Results and discussion

The reactions involved in the formation of β-TCP during the chemical precipitation can be expressed as follows:

$$(NH_4)_2(HPO_4) + 3Ca(NO_3)_2{\times}4H_2O \rightarrow Ca_3(PO_4)_2 + 6NH_4NO_3 + 4H_2O \quad (3)$$

The effect of the solution pH on the composition of the precipitates was investigated by ICP method, and analysis was performed on the precipitates dried at 100°C for 24 h. It can be seen, Table 1, that the Ca/P value was 1.51 and 1.59 when the pH of the precursor solution was 8.0 and 10.8, respectively. The unreacted precursors are believed to be washed out during filtering process.

Figure 2 shows SEM micrograph of the samples A and B after filtering and before calcination. It can be seen that the as-prepared powders consist of aggregated particles with broad size distribution.

*3.1. FTIR spectroscopy*

The FTIR spectrum of the powder prepared at pH = 8 is shown in Fig. 3. The characteristic absorption bands at 3433 and 1631 $cm^{-1}$ are attributed to adsorbed water. The bands at 900–1200 $cm^{-1}$ were the stretching mode of $PO_4^{3-}$ group. The sharp peaks at 561 and 607 $cm^{-1}$ represent the vibration peaks of $PO_4^{3-}$ in β-TCP [19,20].

The FTIR spectrum of the sample B, prepared at pH = 10.8, is shown in Fig. 4. The broad bands at 3433 $cm^{-1}$ and 1642 $cm^{-1}$ were attributed to adsorbed water, while

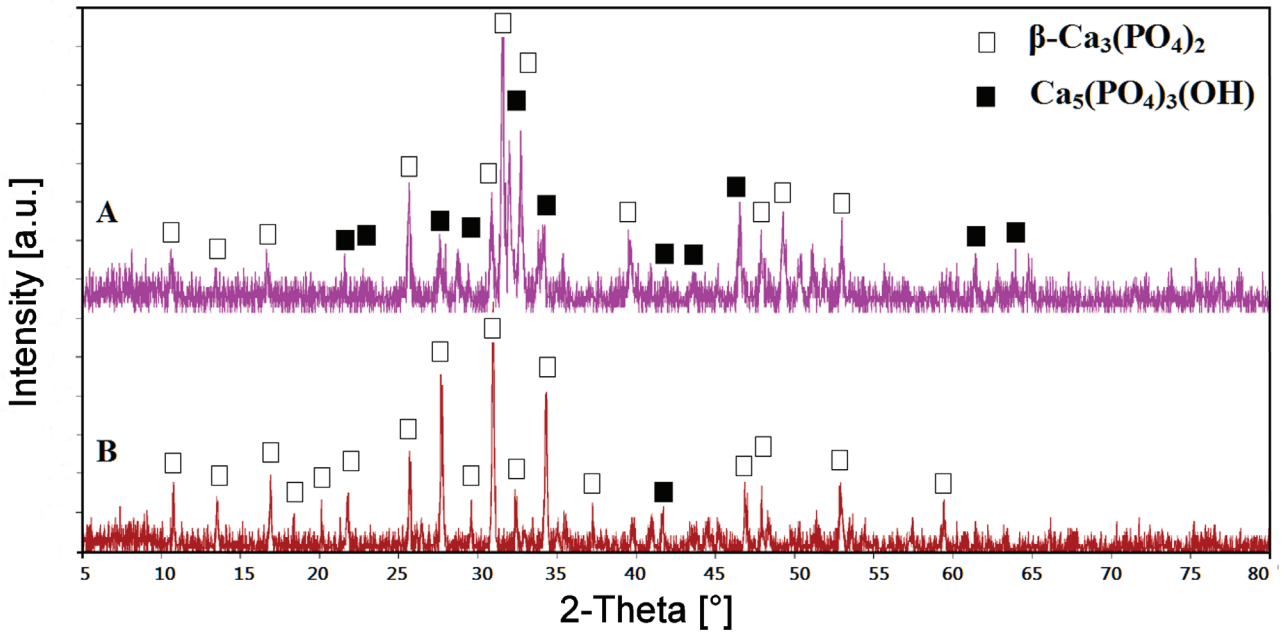


**Figure 5. XRD patterns of β-TCP powders synthesized at pH=8 (A) and pH=10.8 (B)**

sharp peak at 3572 $cm^{-1}$ appeared due to the stretching vibration of the lattice $OH^-$ ions. The peak at 633 $cm^{-1}$ was assigned to the O-H deformation mode. The characteristic bands due to vibration of $PO_4^{3-}$ group appeared at 470, 570, 964 and 1046 $cm^{-1}$. The observation of the asymmetric P-O stretching vibration of the $PO_4^{3-}$ bands at 964 $cm^{-1}$ as a distinguishable peak, together with the sharp peaks at 633, 602 and 570 $cm^{-1}$ correspond to the triply degenerate bending vibrations of $PO_4^3$ in hydroxyapatite. Our FTIR results were similar to the literature data [21–23].

*3.2. XRD analysis*

The XRD analysis was performed using the X-ray diffractometer. The straight base line and sharp peaks of the diffractogram in Fig. 5 confirmed that the products were well crystallized. The XRD pattern in Fig. 5 indicated that the sample A contains mostly β-TCP. On the other side, both crystalline phase (tricalcium phosphate and hydroxyapatite) exist in the sample B. XRD pattern also reveals that the as-dried powder B has a poorly crystallized hydroxyapatite phase. The average crystallite size, determined by Scherrer equation, of the sample A and B is 50 and 80 nm, respectively.

It is important to note that even there are many phases in addition to the hydroxyapatite and β-tricalcium phosphate, which have Ca/P ratios of 5/3 and 3/2, respectively (such as mono-, di-, tri-, and tetra-calcium phosphates), they were not detected in the investigated

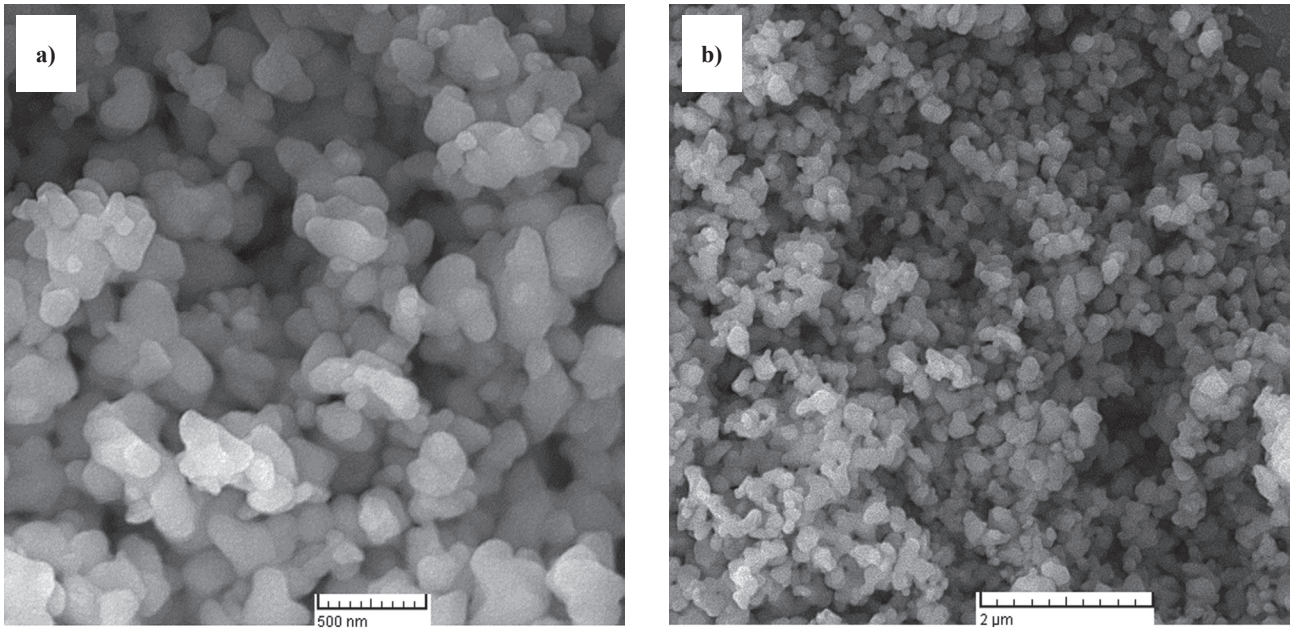


**Figure 6. SEM images of sample A (synthesized at pH = 8) at two different magnifications: a) 50000× and b) 20000×**

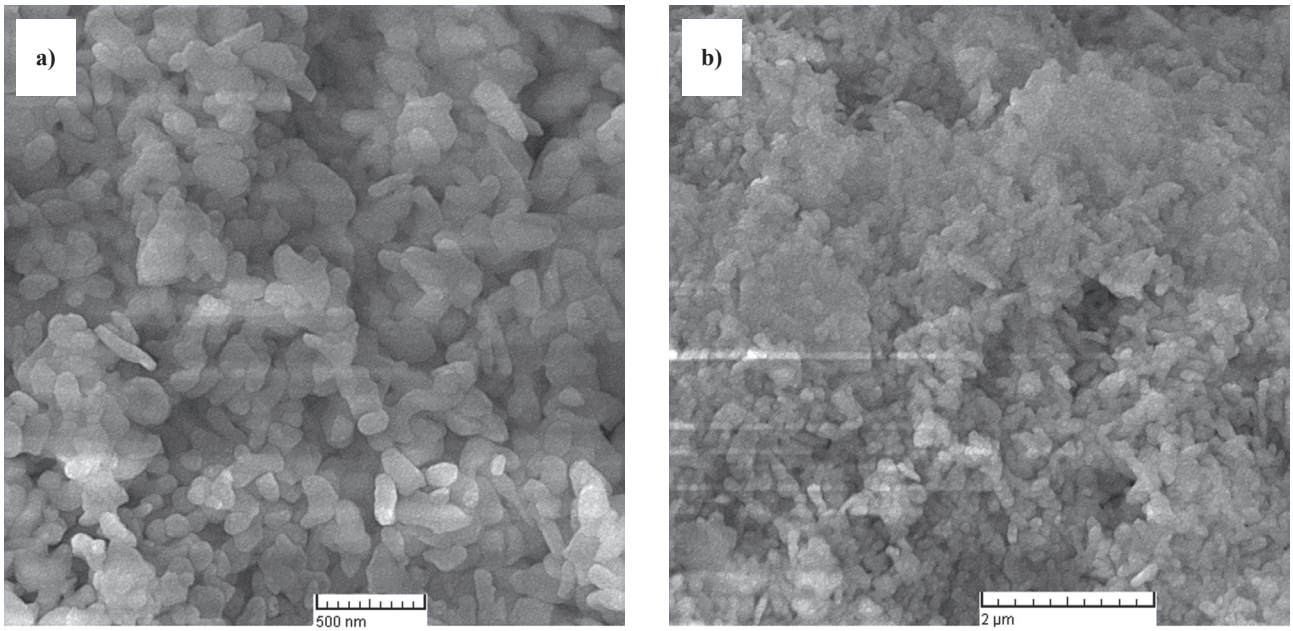


**Figure. 7. SEM images of sample B (synthesized at pH = 10.8) at two different magnifications: a) 50000× and b) 20000×**

powders. Park and Lakes [24] reported that the stability in solution generally increases with increasing Ca/P ratios and that different phases can be used in different applications depending upon whether a degradable or a bioactive material is desired. Thus, our results confirmed that with increasing pH up to 10.8 it is possible to increase the Ca/P ratio to 1.59 and change phase composition of the synthesized powders.

*3.3. SEM analysis*

The morphologies of the TCP powder precipitated at pH = 8 was shown in Fig. 6 at two different magnifications. The TCP powder is highly agglomerated with almost spherical particles having average size of 150 nm. The necking among the particles was apparent due to localized sintering at 700°C. Figure 7 shows aggregates of sample B (synthesized at pH = 10.8) at two different magnifications. The powder is also highly agglomerated, but it consists of smaller particles, 80–150 nm.

## V. Conclusions

In this study, the synthesis of biocompatible nanosized β-TCP powder via wet precipitation method and using calcium and phosphorous precursors is reported. It is shown that high purity products, β-TCP nanopowder and hydroxyapatite/β-TCP composite, could be obtained by this simple process. The sample prepared at pH = 8 is β-TCP powder with Ca/P ratio of 1.51, whereas the powder prepared at pH = 10.8 has hydroxyapatite/β-TCP composite structure and Ca/P ratio 1.59. Thus, our results confirmed that with increasing pH up to 10.8 it is possible to increase the Ca/P ratio to 1.59 and change phase composition of the synthesized powders. The prepared powders could be widely used for biomedical applications.

**Acknowledgements:** The authors are indebted to the Ceramic Laboratory (Institute for Standard and Industrial Research of Iran) that supplied the raw materials for development of this research and to the Ceramic Department (International University of Iran) for its financial support.

## References

1. N. Kivrak, A.C. Tas, "Synthesis of calcium hydroxyapatitetricalcium phosphate (HA-TCP) composite bioceramics powders and their sintering behavior", *J. Am. Ceram. Soc*., **81** (1998) 2245–2252.
2. I.R. Gibson, I. Rehman, S.M. Best, W. Bonfield, "Characterization of the transformation from calcium-deficient apatite to β-tricalcium phosphate", *J. Mater. Sci.: Mater. Med*., **12** (2000) 799–804.
3. K.P. Sanosh, M.C. Chu, A. Balakrishnan, T.N. Kim, S.J. Cho, "Sol-gel synthesis of pure nano sized β-tricalcium phosphate crystalline powders", *Curr. Appl. Phys.*, **10** (2010) 68–71.
4. B. Viswanath, R. Raghavan, N.P. Gurao, U. Ramamurty, N. Ravishankar, "Mechanical properties of tricalcium phosphate single crystals grown by molten salt synthesis", *J. Acta Biomater.*, **4** (2008) 1448–1454.
5. F. Albee, H. Morrison, "Studies in bone growth β-triple calcium phosphate as a stimulus osteogenesis", *J. Ann. Surg.*, **71**(1920) 32–39.
6. L.L. Hench, "Bioceramics", *J. Am Ceram. Soc.*, **81** (1998) 1705–1728.
7. P.N. De Aza, P. Pena, "Bioactive glasses and glass-ceramics", *J. Bol. Soc. Esp. Ceram. Vidr*., **46** (2007) 45–55.
8. S. Roy, B. Basu, "Mechanical and tribological characterization of human tooth", *J. Mater. Charact.*, **59** (2008) 747–756.

9. J.H. Welch, J.H. Gutt, "High-temperature studies of the system calcium oxide–phosphorus pentoxide", *J. Chem. Soc.*, **29** (1961) 4442–4444.
10. R.G. Carrodeguas, A.H. De Aza, I. Garcia-Paez, S. De Aza, P. Pena, "Revisiting the phase-equilibrium diagram of the $Ca_3(PO_4)_2$-$CaMg(SiO_3)_2$ system", *J. Am. Ceram. Soc.*, **93** (2010) 561–569.
11. K. de Groot, "Clinical applications of calcium phosphate biomaterials: A review", *Ceram. Int.*, **19** [5] (1993) 363–366.
12. S. Metsger, T.D. Driskell, J.R. Paulsrud, "Tricalcium phosphate ceramic - a restorable bone implant: review and current status", *J. Am. Dent. Assoc.*, **105** (1982) 1035–1038.
13. K. Lin, J. Chang, J. Lu, W. Wu, Y. Zeng, "Properties of β-$Ca_3(PO_4)_2$ bioceramics prepared using nano-size powders", *Ceram. Int*., **33** (2007) 979–985.
14. J.S. Bow, S.C. Liou, S.Y. Chen, "Structural characterization of room-temperature synthesized nano-sized β-tricalcium phosphate", *Biomater.*, **25** (2004) 3155–3161.
15. F. Zhang, K. Lin, J. Chang, J. Lu, C. Ning, "Spark plasma sintering of macroporous calcium phosphate scaffolds from nanocrystalline powders", *J. Eur. Ceram. Soc.*, **28** (2008) 539–545.
16. A. El-Ghannam, "Bone reconstruction: from bioceramics to tissue engineering", *J. Expert. Rev. Med. Devices*, **2** (2005) 87–101.
17. L.A. Bauer, N.S. Birenbaum, G.J. Meyer, "Biological applications of high aspect ratio nanoparticles", *J. Mater. Chem.*, **14** (2004) 517–526.
18. L.A. Azaroff, *Elements of X-ray Crystallography, McGraw-Hill*, New York, 1968. pp. 38–42.
19. C. Biqin, Z. Zhaoquan, Z. Jingxian, L. Qingling, J. Dongliang, "Fabrication and mechanical properties of β-TCP pieces by gelcasting method", *Mater. Sci. Eng*. C, **28** (2008) 1052–1056.
20. S. Raynaud, E. Champion, D. Bernache-Assollant, P. Thomas, "Calcium phosphate apatites with variable Ca/P atomic ratio I. Synthesis, characterization and thermal stability of powders", *Biomater*., **23** (2002) 1065–1072.
21. W. Aili, L. Dong, Y. Hengbo, W. Huixiong, W. Yuji, R. Min, J. Tingshun, C. Xiaonong, X. Yiqing, "Size-controlled synthesis of hydroxyapatite nanorods by chemical precipitation in the presence of organic modifier", *Mater. Sci. Eng*., **27** (2007) 865–869.
22. R. Murugan, S. Ramakrishna, "Bioresorbable composite bone paste using polysaccharide based nano hydroxyapatite", *J. Biomater.*, **25** (2004) 3829–3835.
23. W. Li, L. Yue, L. Chunzhong, "In situ processing and properties of nanostructured hydroxyapatite/alginate composite", *J. Nanopart. Res*., **11** (2009) 691–699.
24. J. Park, R.S. Lakes, *Biomaterials, An Introduction*, 2nd ed., Plenum Press, New York, 1992.